Widely tunable microwave phase shifter based on silicon-on-insulator dual-microring resonator

Pu, Minhao; Liu, Liu; Xue, Weiqi; Ding, Yunhong; Ou, Haiyan; Yvind, Kresten; Hvam, Jørn Märcher

Published in:
Optics Express

Link to article, DOI:
10.1364/OE.18.006172

Publication date:
2010

Document Version
Publisher's PDF, also known as Version of record

Widely tunable microwave phase shifter based on silicon-on-insulator dual-microring resonator

Minhao Pu,[1]* Liu Liu[1], Weiqi Xue[1], Yunhong Ding[1,2], Haiyan Ou[1], Kresten Yvind[1], and Jørn M. Hvam[1]

[1]*DTU Fotonik, Department of Photonics Engineering, Technical University of Denmark, Build. 343, DK-2800 Kongens Lyngby, Denmark*

[2]*Wuhan National Laboratory for Optoelectronics, Huazhong University of Science and Technology, Wuhan, 430074, China*

*mipu@fotonik.dtu.dk

Abstract: We propose and demonstrate tunable microwave phase shifters based on electrically tunable silicon-on-insulator microring resonators. The phase-shifting range and the RF-power variation are analyzed. A maximum phase-shifting range of 0~600° is achieved by utilizing a dual-microring resonator. A quasi-linear phase shift of 360° with RF-power variation lower than 2dB and a continuous 270° phase shift without RF-power variation at a microwave frequency of 40GHz are also demonstrated.

OCIS codes: (350.4010) Microwaves; (060.5625) Radio frequency photonics; (130.3120) Integrated optics devices; (230.5750) Resonators.

References and links

1. J. Capmany, and D. Novak, "Microwave photonics combines two worlds," Nat. Photonics **1**(6), 319–330 (2007).
2. S. Tonda-Goldstein, D. Dolfi, A. Monsterleet, S. Formont, J. Chazelas, and J. P. Huignard, "Optical signal processing in radar systems," IEEE Trans. Microw. Theory Tech. **54**(2), 847–853 (2006).
3. J. Capmany, B. Ortega, D. Pastor, and S. Sales, "Discrete-time optical processing of microwave signals," J. Lightwave Technol. **23**(2), 702–723 (2005).
4. M. Fisher, and S. Chuang, "A microwave photonic phase-shifter based on wavelength conversion in a DFB laser," IEEE Photon. Technol. Lett. **18**(16), 1714–1716 (2006).
5. A. Loayssa, and F. J. Lahoz, "Broad-band RF photonic phase shifter based on stimulated Brillouin scattering and single-sideband modulation," IEEE Photon. Technol. Lett. **18**(1), 208–210 (2006).
6. W. Xue, S. Sales, J. Capmany, and J. Mørk, "Microwave phase shifter with controllable power response based on slow- and fast-light effects in semiconductor optical amplifiers," Opt. Lett. **34**(7), 929–931 (2009).
7. W. Xue, Y. Chen, F. Öhman, S. Sales, and J. Mørk, "Enhancing light slow-down in semiconductor optical amplifiers by optical filtering," Opt. Lett. **33**(10), 1084–1086 (2008).
8. M. Povinelli, S. Johnson, and J. Joannopoulos, "Slow-light, band-edge waveguides for tunable time delays," Opt. Express **13**(18), 7145–7159 (2005), http://www.opticsinfobase.org/oe/abstract.cfm?URI=oe-13-18-7145.
9. L. Wei, W. Xue, Y. Chen, T. T. Alkeskjold, and A. Bjarklev, "Optically fed microwave true-time delay based on a compact liquid-crystal photonic-bandgap-fiber device," Opt. Lett. **34**(18), 2757–2759 (2009).
10. Q. Chang, Q. Li, Z. Zhang, M. Qiu, T. Ye, and Y. Su, "A Tunable Broadband Photonic RF Phase Shifter Based on a Silicon Microring Resonator," IEEE Photon. Technol. Lett. **21**(1), 60–62 (2009).
11. M. Pu, L. Liu, W. Xue, Y. Ding, L. H. Frandsen, H. Ou, K. Yvind, and J. M. Hvam, "Tunable Microwave Phase Shifter Based on Silicon-on-Insulator Microring Resonator," submitted to IEEE Photon. Technol. Lett.
12. J. Capmany, B. Ortega, and D. Pastor, "A Tutorial on Microwave Photonic Filters," J. Lightwave Technol. **24**(1), 201–229 (2006).
13. W. Xue, S. Sales, J. Mork, and J. Capmany, "Widely Tunable Microwave Photonic Notch Filter Based on Slow and Fast Light Effects," IEEE Photon. Technol. Lett. **21**(3), 167–169 (2009).
14. J. Heebner, A. Vincent Wong, A. Schweinsberg, R. W. Boyd, and D. J. Jackson, "Optical transmission characteristics of fiber ring resonators," IEEE J. Quantum Electron. **40**(6), 726–730 (2004).
15. T. Shoji, T. Tsuchizawa, T. Watanabe, K. Yamada, and H. Morita, "Low loss mode size converter from 0.3μm square Si wire waveguides to single mode fibres," Electron. Lett. **38**(25), 1669–1670 (2002).
16. M. Pu, L. H. Frandsen, H. Ou, K. Yvind, and J. M. Hvam, "Low Insertion Loss SOI Microring Resonator Integrated with Nano-Taper Couplers," The Conference on Frontiers in Optics (FiO) 2009, FThE1 (2009).

1. Introduction

Microwave photonics has lately received increasing interests [1]. Microwave systems can benefit from the characteristics of photonic semiconductor components such as compact size,

#122999 - $15.00 USD Received 25 Jan 2010; revised 26 Feb 2010; accepted 3 Mar 2010; published 11 Mar 2010

large bandwidth, fast tunability, immunity to electromagnetic interference and low weight. Microwave phase shifters are key components in many microwave applications, such as phased-array antennas [2] and microwave filters [3]. So far, several schemes for phase shifting have been reported [4–11]. For instance, a phase shift of 110° with 6dB RF power variation was obtained by using a distributed-feedback (DFB) laser through wavelength conversion [4], Based on stimulated Brillouin scattering (SBS) in an optical fiber, a phase shift of 360° was achieved with less than 3dB RF power variation [5]. Two semiconductor optical amplifiers (SOAs) were cascaded to realize a phase shifting range of 0~240° with controllable RF power response based on slow-light effects [6,7]. A photonic-crystal fiber device was used as a phase shifter with a tuning range of 0~70° caused by band-edge effects [8,9]. Recently, silicon-on-insulator (SOI) microring resonators (MRRs) have also been used as phase shifters [10,11]. A shifting range of 0-260° was obtained with thermo-optic tuning from a high-power control light [10]. Previously, we also demonstrated an electrically tunable phase shifter based on one MRR with a phase-shifting range of 0-336° in [11]. However, it is difficult to realize a full 360° phase shift by using a single MRR. This limits its practical applications in microwave systems since many applications, such as microwave photonic filters [12,13], require phase shifters with a full 360° tuning range. In addition, the RF power varies dramatically during the phase shifting operation [11] which also hampers the applications.

In this paper, we propose and demonstrate a microwave phase shifters based on a dual-microring resonator (DMRR), which employs two cascaded MRRs with independent, electrically controllable, micro heaters. The RF phase-shifting range and the RF-power variation are analyzed for the proposed phase shifter. A maximum phase-shifting range of 0~600° is achieved by utilizing a DMRR. A quasi-linear phase shift of 360° with ~2dB RF-power variation and a continuous 270° phase shift without noticeable RF-power variation at a microwave frequency of 40GHz are also demonstrated. These devices can be easily integrated with photonic and electronic circuits.

2. Design

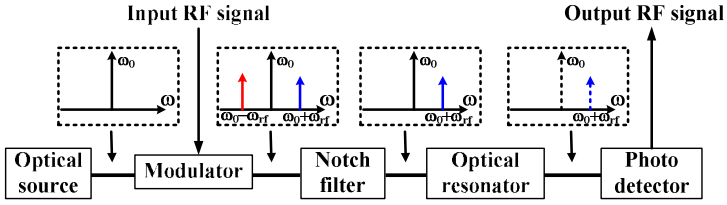

Fig. 1. Schematic layout of an RF phase shifter

Figure 1 shows the schematic layout of an RF phase shifter. The RF signal is imprinted on an optical signal via an external modulator generating an optical signal composed of a strong carrier at ω_0 and two major sidebands, red-shifted and blue-shifted by the RF frequency ωrf. A notch filter is used to filter out one of the sidebands and then the optical signal with two frequency components is sent to the optical resonator (here an MRR). The optical field input to the optical resonator can be expressed as

$$E(t) = A_0 \exp(j\omega_0 t) + A_1 \exp[j(\omega_0 + \omega_{rf})t] \quad (1)$$

where A_0 and A_1 are the amplitudes of the two frequency components of the optical signal. The output field after the optical resonator can be therefore expressed as

$$E'(t) = A_0 A'_0 \exp(j\omega_0 t)\cdot\exp(j\theta_0) + A_1 A'_1 \exp[j(\omega_0 + \omega_{rf})t]\cdot\exp(j\theta_1) \quad (2)$$

where A'_0, A'_1 and θ_0, θ_1 are the amplitude transmission gain and the induced optical phase shift at the corresponding frequencies for the MRR, respectively. Finally, the output optical

#122999 - $15.00 USD Received 25 Jan 2010; revised 26 Feb 2010; accepted 3 Mar 2010; published 11 Mar 2010

signal is detected by a photo detector (PD) and the RF component of the output signal from PD is

$$i_{AC}(t) \propto \Re A_0 A'_0 A_1 A'_1 \cos[\omega_{rf} t + (\theta_0 - \theta_1)] \tag{3}$$

where $\Re$ is the responsivity of the PD. The phase of the output RF signal is therefore determined by the optical phase difference θ_0-θ_1. And if the resonance of the optical resonator can be tuned (between the two optical frequencies) to change the two optical phases, the phase difference can be varied and then realize the RF phase shift.

2.1 Phase shifter based on a single microring resonator (MRR)

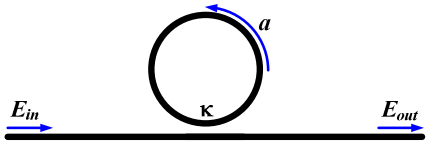

Fig. 2. Schematic of an all-pass single MRR.

Figure 2 shows the schematic drawing of an all-pass single MRR, where κ and *a* are the amplitude coupling coefficient of the coupling region and roundtrip amplitude transmission coefficient, respectively. The transmittance of the complex field at the through port can be expressed as

$$\frac{E_{out}}{E_{in}} = \frac{r - ae^{j\phi}}{1 - are^{j\phi}} \tag{4}$$

where φ is the roundtrip phase change of the ring, which is related to the optical frequency, and r is the amplitude transmission coefficient of the coupling region which satisfies the relation $r^2+\kappa^2=1$ for lossless coupling. The phase shift of the transmitted light can be derived as [14]

$$\Phi = \pi + \phi + \tan^{-1}\frac{r\sin\phi}{a - r\cos\phi} + \tan^{-1}\frac{ar\sin\phi}{1 - ar\cos\phi} \tag{5}$$

Figures 3(a) and 3(b) show the optical intensity transmission and phase shift at the through port of the MRR with different amplitude coupling coefficients κ. Here, we assume the diameter of the SOI MRR is 35μm and the effective group index of the SOI waveguide is 4.26 which correspond to a free spectral range (FSR) of 640GHz. The propagation loss of the SOI waveguide composing the ring is assumed to be 2dB/cm. As shown in Fig. 3(b), the phases experience monotonically a full 360° phase shift from negative to positive detuning with different curve shapes. If an optical signal carrying a microwave signal with two frequency components, i.e. a carrier frequency ω_0 and one sideband frequency $\omega_0 + \omega_{rf}$, is input to the MRR, the phase difference of the two frequency components can be changed in different ways depending on the value of the coupling coefficient κ of the MRR. In other words, the RF phase-shifting performance will be different for the MRRs with different coupling coefficients. Figures 3(c) and 3(d) show the RF power and RF phase shift, respectively, for the MRRs as a function of detuning of the resonance frequency (ω_{MRR}) from the carrier frequency (ω_0) over an FSR tuning range. Here, we assume the RF frequency (ω_{rf}) is 40GHz. It is clear that the maximum RF phase-shifting range increases as the amplitude coupling coefficient decreases which results in higher quality (Q)-factor of the MRR [see Fig. 3(d)]. The RF power variation also increases with lower coupling coefficient (higher Q-factor) for the MRR as illustrated in Fig. 3(c). The RF phase-shifting range can be further increased, though, for the larger amplitude coupling coefficients by increasing the RF frequency, as shown in Fig. 3(e). The higher Q-factor MRR with lower coupling coefficient is always

#122999 - $15.00 USD Received 25 Jan 2010; revised 26 Feb 2010; accepted 3 Mar 2010; published 11 Mar 2010

preferred if a large RF phase shifting range is expected. However, a full 360° RF phase shift is still difficult to realize through a single MRR [Fig. 3(d)], although the optical phases for all the MRRs experience a 360° change [Fig. 3(b)], and the increased RF power variation would become unbearable when a higher Q-factor MRR is employed [Fig. 3(c)]. In our previous experimental demonstration [11], a phase shifting range of 0~336° was achieved by using a single MRR with Q-factor of 28,000. However, the RF-power variation amounted to 11dB.

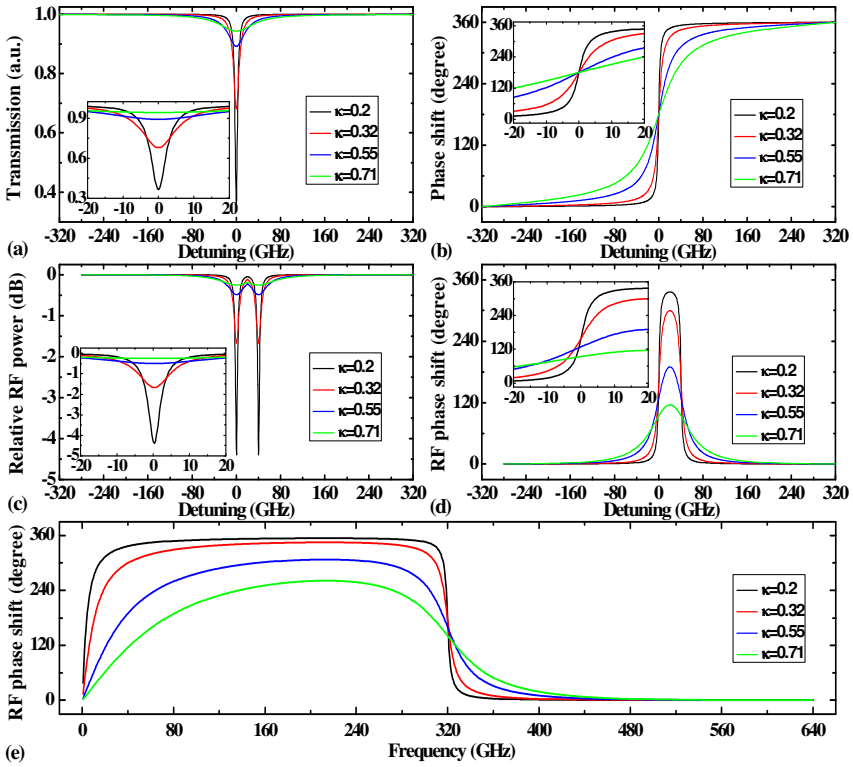

Fig. 3. Optical intensity transmission (a) and phase shift (b) as a function of the detuning (ω-ω_{MRR}) at the through port for the MRRs with different coupling coefficients κ. RF power (c) and RF phase shift (d) for the MRRs as a function of the detuning (ω_{MRR}-ω_0) at a RF frequency of 40GHz with different coupling coefficients κ. All the insets are the zoomed view for a detuning range from –20GHz to 20GHz. (e) The maximum RF phase shift versus the RF frequency for the MRRs with different coupling coefficients κ.

2.2 Phase shifter based on dual-microring resonator (DMRR)

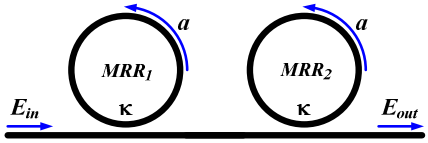

Fig. 4. Schematic of an all-pass DMRR.

Figure 4 shows the schematic drawing of an all-pass dual-microring resonator (DMRR). The two cascaded rings are designed to have the same nominal geometries. Here, we also assume that an optical signal with two frequency components (ω_0 and $\omega_0+\omega_{rf}$) is injected to the DMRR. The diameter of the two MRRs and the RF frequency are 35μm and 40GHz, respectively. Figure 5 illustrates the optical intensity transmission, the RF power, the optical

#122999 - $15.00 USD Received 25 Jan 2010; revised 26 Feb 2010; accepted 3 Mar 2010; published 11 Mar 2010

phase shift and the RF phase shift for the DMRR at the through port with different resonance offsets (ω_{MRR2}-ω_{MRR1}) between the two MRRs. A total optical phase shift of 720° can be achieved for the DMRR. As shown in Figs. 5(a) and 5(c), the transmission spectrum and the phase curve can be altered by offsetting the resonances for the two MRRs. When the resonance offset increases from 0 to 3GHz, the notch bandwidth increases, with a reduced notch depth, and the bottom of the notch becomes flat. As the resonance offset increases further, the notch splits into two notches while the phase curve acquires a step-like shape. The RF power and RF phase shift behave in a similar way, as shown in Figs. 5(b) and 5(d). Therefore, the resonance offset can be tuned to a desired value (e.g., 3GHz in this case) to obtain a wide notch bandwidth, a decreased notch depth and a flattened notch bottom, and if the RF phase shifter is operated within this flat regime, one can realize an RF phase shift in a certain range with minimal RF power variation since the RF power follows the optical power. The insets in Figs. 5(b) and 5(d) show the zoomed views for the RF phase shift and RF power variation, respectively, in the detuning range from −1GHz to 4GHz for the DMRR with a fixed resonance offset of 3GHz. One can find that a quasi-linear phase-shifting range of 360° can be obtained with less than 2.4dB RF power variation. A tuning range of 90° with negligible RF-power variation can also be found within the detuning regime from 0.95GHz to 1.92GHz. Compared with the phase shifter based on single MRRs [see insets in Figs. 3(c) and 3(d)], the DMRR-based phase shifter offers a larger phase shifting range, a more linear phase shift of 360° together with a much lower RF power variation. The bandwidth of the flat bottom regime can be further increased by a careful design of the Q-factor of each MRR and an optimal resonance offset between the MRRs, resulting in an increase of the tuning range with constant RF power.

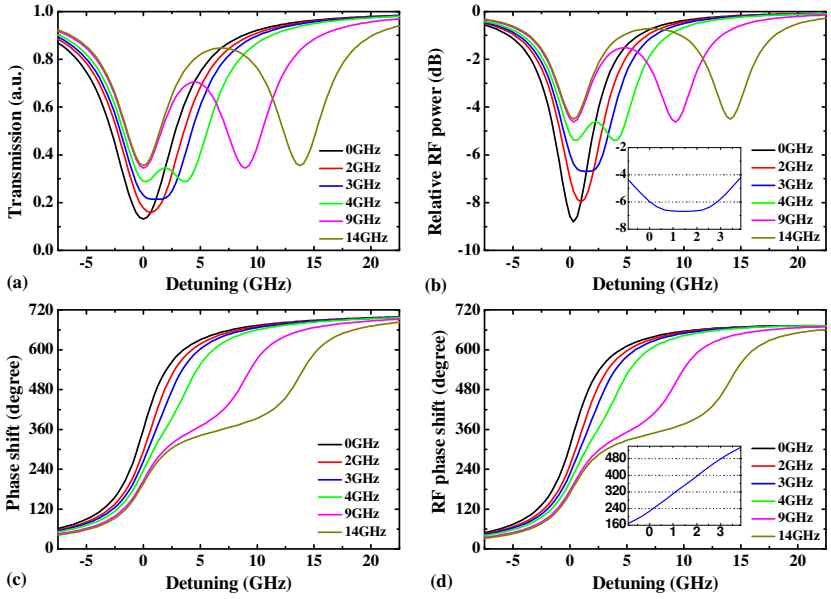

Fig. 5. Optical intensity transmission (a) and phase shift (c) as a function of the detuning (ω-ω_{MRR1}) for the DMRR with different resonance offsets (ω_{MRR2}-ω_{MRR1}). RF power (b) and RF phase shift (d) as a function of the detuning (ω_{MRR1}-ω_0) at an RF frequency of 40GHz. Insets are zoomed views for the DMRR with 3GHz resonance offset for a detuning range from −1GHz to 4GHz. Here, κ^2, a^2 are always assumed to be 0.04 and 0.995, respectively.

In the above analysis, we fixed the resonance offset of the two MRRs. We can also suppress the RF power variation over a larger tuning range by varying the resonance offset during the phase-shifting operation since the two cascaded MRRs are designed to be tuned independently. Figure 6(a) shows the RF phase shift and the RF power as a function of detuning of resonance frequencies (ω_{MRR1} and ω_{MRR2}) from the optical carrier frequency (ω_0)

#122999 - $15.00 USD Received 25 Jan 2010; revised 26 Feb 2010; accepted 3 Mar 2010; published 11 Mar 2010

for the DMRRs with power coupling coefficient $\kappa^2 = 0.04$. One can find that there are regions where the contour lines for RF phase shift (color-shaded contours) and RF power variation (black-curve contours) are not parallel. Therefore, the RF phase shift and the RF power can be tuned independently to some extent. If the tuning of the resonances of the two MRRs can be controlled in such a way that one of the contour lines for RF power is followed, there would be no RF power variation in the phase shifting process. For instance, if we follow the −6dB power contour curve, a continuous phase shifting range of ~280° can be obtained. The maximum continuous RF phase shifting range without power variation depends on the Q-factor of each MRR. The performance of a phase shifter based on a DMRR with a higher power coupling coefficient of 0.3 (lower Q-factor) is also illustrated in Fig. 6(b). Although the operating RF power level becomes higher and less sensitive to the detuning of the resonances, the maximum phase shifting range that can be achieved following one contour line is decreased to ~190°. Figure 7 shows the maximum RF phase-shifting range without power variation and the operating RF power level as a function of power coupling coefficient κ^2 of the DMRR. It is obvious that the phase shifter based on higher Q-factor DMRR (lower coupling coefficient) offers larger tuning range without power variation at the expense of an increased overall RF-power loss. Since the absolute operating RF power is of less importance for such a microwave phase shifter, we conclude that a DMRR with high Q-factor is more preferable in this case.

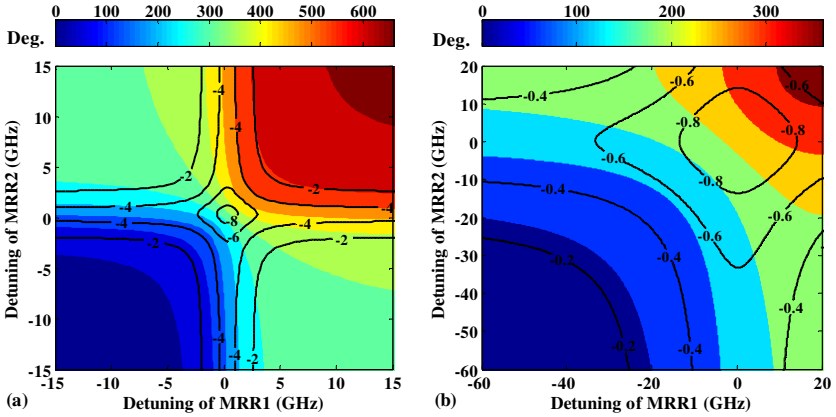

Fig. 6. Contour plots of RF phase shift for a 40GHz signal (in degrees, color-shaded contours) and RF power (in decibels, black-curve contours) as a function of the detuning of resonance frequencies (ω_{MRR1} and ω_{MRR2}) from the optical carrier frequency (ω_0) for tdhe DMRRs with power coupling coefficient κ^2 of 0.04 (a) and 0.3 (b), respectively.

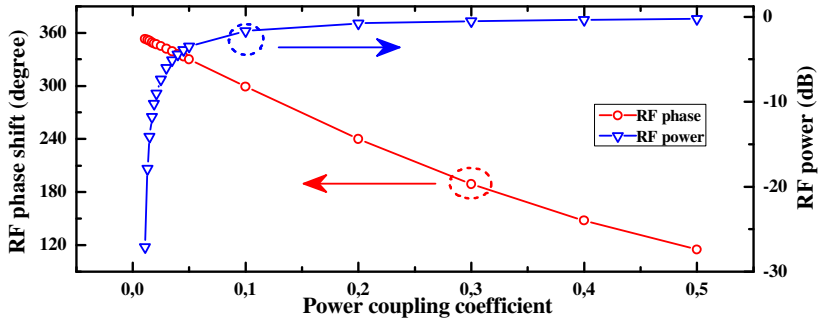

Fig. 7. Maximum RF phase shift and RF power level for constant-power operation as a function of the power coupling coefficient κ^2.

#122999 - $15.00 USD Received 25 Jan 2010; revised 26 Feb 2010; accepted 3 Mar 2010; published 11 Mar 2010

3. Fabrication

Figure 8(a) shows the schematic diagram of a tunable MRR. The tunable MRR was fabricated in an SOI wafer with a top silicon thickness of 250nm and a 3-μm buried silicon dioxide. Diluted (1:1 in anisole) electron-beam resist ZEP520A was spin-coated on the wafer to create a ~110-nm thick masking layer. The microring structure was defined in the ZEP520A layer with electron-beam lithography (JEOL JBX-9300FS). The patterns were subsequently transferred to the top silicon layer with inductively coupled plasma reactive ion etching. Then a 550-nm thick benzocyclobuten (BCB) top cladding was spin-coated and subsequently hard-cured. After that, 400nm of ZEP520A resist and electron-beam lithography were employed again to define the pattern of the micro heater. Evaporation and lift-off techniques were used as the last steps to form 100-nm thick titanium heaters together with contact pads. Figure 8(b) shows an optical microscope picture of the fabricated single MRR with micro heater. The waveguide width is 450nm and the diameter of the microring is 35μm. The heater width in the ring area is 1μm. At both ends of the device, the waveguide is tapered from 450nm to 4μm to expand the guided mode for more efficient fiber-to-chip coupling. The insertion loss of the device is ~15dB, where we estimate the fiber to waveguide coupling loss to account for ~14dB. This loss can be lowered down to ~2dB using suitable mode converters [15,16].

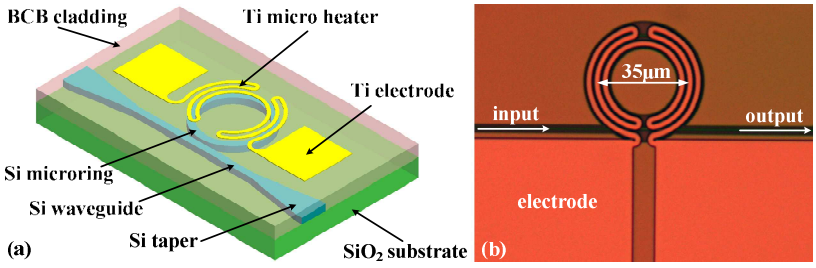

Fig. 8. (a) Schematic diagram of the tunable MRR with micro heater. (b) Top-view microscope picture of the fabricated tunable MRR with micro heater.

To test the tunability of MRR by applying electrical current on micro heater, we use a single MRR with a coupling gap (ring-to-waveguide gap) of 200nm between the ring and straight waveguide. Figure 9(a) shows the measured transmission spectra for the MRR with different applied electrical powers. The 3-dB bandwidth of the resonant notch is 0.1nm which corresponds to a Q-factor of ~15,500. The resonance red-shifts linearly as the applied power increases as shown in Fig. 9(b). An electrical power of ~40mW is required for the resonance shifting range of a whole FSR, and the maximum achieved resonance shift is ~8nm with this design.

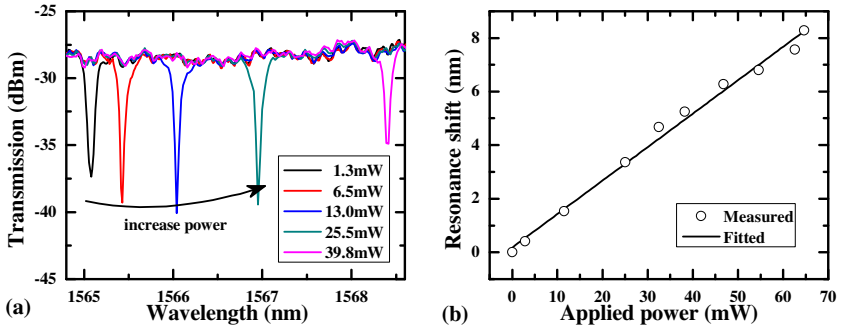

Fig. 9. (a) Measured transmission spectrum with different applied power on the micro heater for the MRR. (b) Measured resonance shift versus the applied power on the micro heater.

#122999 - $15.00 USD Received 25 Jan 2010; revised 26 Feb 2010; accepted 3 Mar 2010; published 11 Mar 2010

4. Experiment setup

The experimental setup used to measure the fabricated device is shown schematically in Fig. 10(a). Light from a tunable laser source (TLS) was modulated through a Mach-Zehnder modulator (MZM) by a microwave signal from the network analyzer. A fiber Bragg grating (FBG) notch filter was used to filter out one sideband of the modulated signal. After that, the optical signal, with the envelope modulated at the microwave frequency in the time domain (i.e., with two peaks of the desired frequency spacing in the spectral domain [see Fig. 11 (b)]) was generated and sent into the fabricated sample as shown in Fig. 10(b). The coupling gaps between the two microrings and the straight waveguide are 150nm which corresponds to a power coupling coefficient of 0.16. The transmission spectrum can be altered by applying current to one of the micro heaters (i.e., the micro heater for MRR_1 [see Fig. 11(a)]). In the measurement, we applied 0.8mW initially on MRR_1 to get a suitable resonance offset between the two MRRs. The polarization of the input light was adjusted to the quasi transverse-electrical (TE) mode by a fiber polarization controller (PC). By adding extra power equally to both micro heaters simultaneously, the resonance frequency of the DMRR can be tuned together with respect to one of the peaks of the optical signal, as illustrated in Fig. 11(b), and then the phase difference between the two peaks is changed. Amplified by an erbium-doped fiber amplifier (EDFA), the output signal was detected by a high-speed photo detector (PD), and converted to the microwave signal. The network analyzer was then used to extract the information of phase and power variations of the microwave signal.

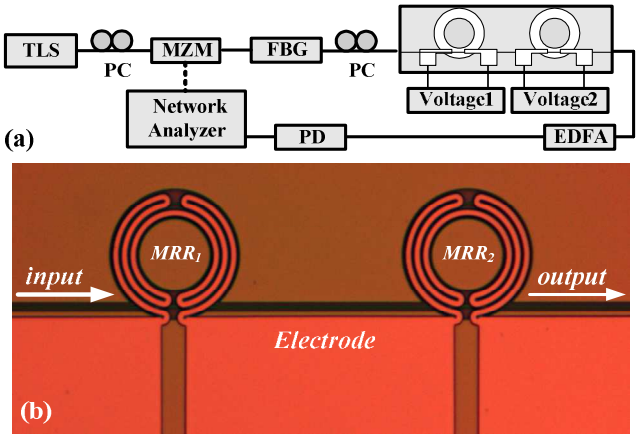

Fig. 10. (a) Experimental setup for phase-shift measurements. (b) Optical microscope picture of the fabricated dual-microring resonator with micro heater.

#122999 - $15.00 USD Received 25 Jan 2010; revised 26 Feb 2010; accepted 3 Mar 2010; published 11 Mar 2010

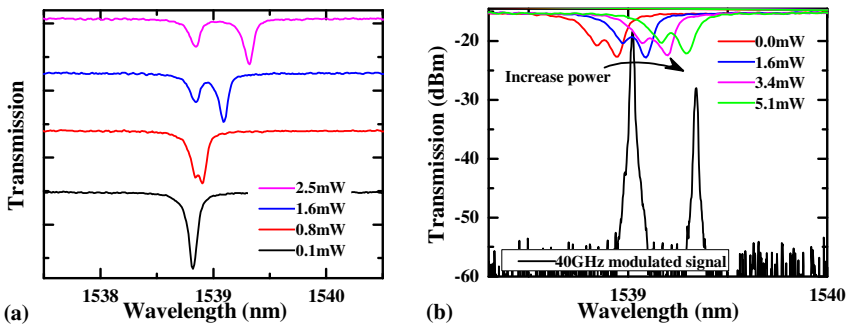

Fig. 11. (a) Measured transmission spectrum of the DMRR with different applied power on the micro heater for MRR_1. (b) Measured transmission spectrum of the DMRR with additional applied power on both micro heaters (see the color curves) and the generated 40GHz microwave signal with carrier wavelength of 1539nm (see the black curve). Here, 0.8mW power is initially applied on micro heater for MRR_1.

5. Experimental results

The measured RF phase shift and RF power variation for a 40GHz microwave carrier as a function of the applied electrical power on both micro heaters are shown in Fig. 12(a). A continuously tunable RF phase shift is demonstrated, and the maximum RF phase shift of 540° is achieved with the RF power variation of ~4dB. However, if the device is operated within the gray region shown in Fig. 12(a), one can obtain not only a quasi-linear phase shift of 360°, but also an RF power variation of only 2dB. In this case, the total required electrical power for phase tuning is ~2mW. As compared to the single-MRR based device in our previous demonstration [11], not only a larger and more linear RF phase shift is achieved, but also the RF power variation is largely suppressed. Figure 12(b) also shows the measured result for another DMRR with a smaller coupling gap of 100nm (larger power coupling coefficient $\kappa^2 = 0.33$) which corresponds to a lower Q-factor. For this measurement, the reference power applied to the micro heater for the MRR_1 was set to 0.5mW to get a suitable fixed resonance offset between the MRRs. A phase shift of 390° is still achieved as shown in Fig. 12(b). Although the maximum phase shift is reduced from 540° to 390° and the total required heating power is increased to ~8.5mW, the total RF power variation in the whole tuning range is only 1dB which is much smaller than that of the high-Q device. Figures 12(c) and 12(d) show the measured maximum RF phase shift and maximum RF power drop, respectively, for the DMRRs with different power coupling coefficients (different Q-factors). The DMRR with higher Q-factor (smaller power coupling coefficient) provides larger RF phase shifting range together with larger RF power variation as shown in Figs. 12(c) and 12(d), which complies with the simulation results. The maximum phase shifting range of 0~600° was achieved by using a DMRR with a coupling gap of 175nm which corresponds to a power coupling coefficient of 0.11.

#122999 - $15.00 USD Received 25 Jan 2010; revised 26 Feb 2010; accepted 3 Mar 2010; published 11 Mar 2010

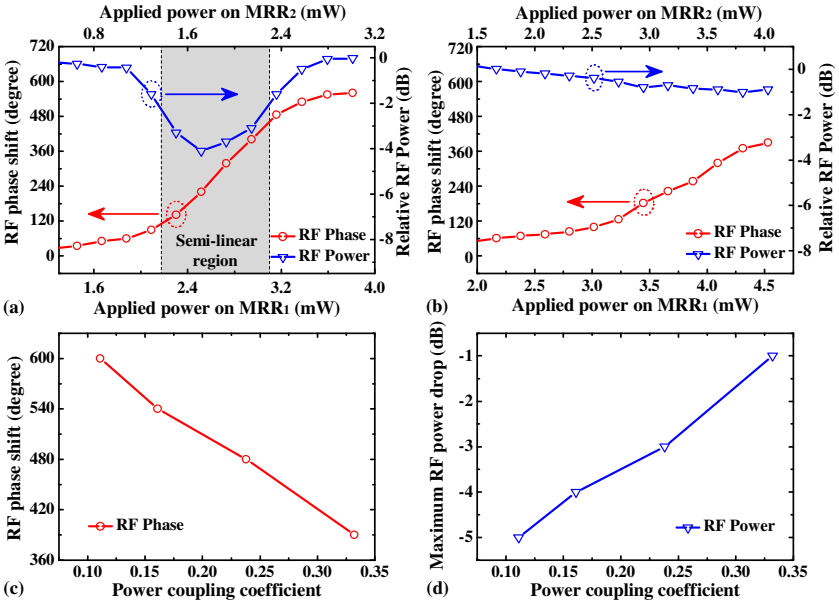

Fig. 12. Measured RF phase shift and RF power versus the power applied to the two micro heaters for the DMRR with a coupling gap of 150nm (a) and 100nm (b). Measured maximum RF phase shift (c) and RF power drop (d) for the DMRRs with different power coupling coefficients.

Figures 13(a) and 13(b) present the measured RF phase shift and RF power as a function of the applied power on the micro heaters for MRR_1 and MRR_2 of the DMRRs with a coupling gap of 150nm and 100nm, respectively. The dotted lines in both figures show the phase shifting operations in the previous measurements with fixed resonance-offsets. One can find that this is not the optimal way to suppress the RF power variation. The applied power on the micro heaters for MRR_1 and MRR_2 can be adjusted independently along a power contour line [i.e., the upper −2dB solid contour line in Fig. 13(a)] to realize the phase shifting. As shown in Fig. 13(a), a phase-shifting range from 180° to 450° can be obtained in this way without noticeable RF power variation for the DMRR. And if we can tolerate 1dB RF-power variation, we can obtain a continuous full 360° phase shift when operation is performed within the region defined by the two upper contour lines of −2dB and −3dB [Fig. 13(a)]. For the DMRR with lower Q-factor (narrower coupling gap), the maximum phase shifting range without power variation is smaller, just as the theoretical prediction mentioned in subsection 2.2.

#122999 - $15.00 USD Received 25 Jan 2010; revised 26 Feb 2010; accepted 3 Mar 2010; published 11 Mar 2010

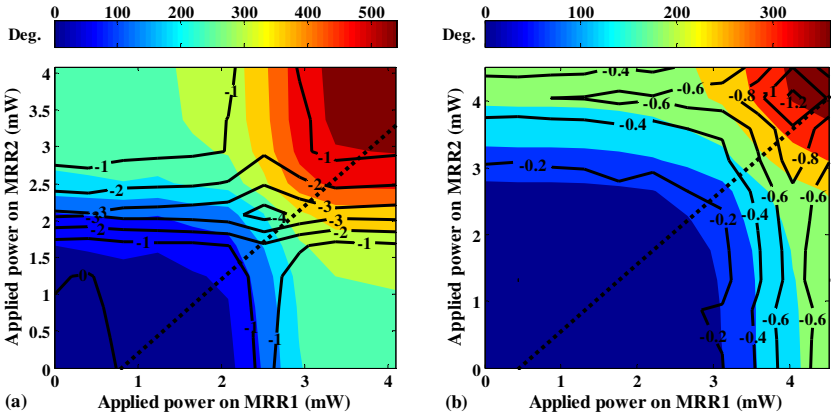

Fig. 13. Contour plots of measured RF phase shift (in degrees, color-shaded contours) and RF power (in decibels, black-curve contours) as a function of the powers applied to the two micro heaters for the DMRR with a coupling gap of 150nm (a) and 100nm (b). The dotted lines represent the RF phase shifting operations in Figs. 12(a) and 12(b), respectively.

6. Conclusion

In conclusion, we have proposed and demonstrated microwave phase shifters based on electrically tunable SOI DMRRs which are composed of cascaded rings with independently controllable micro heaters. For a fixed resonance offset operation, a maximum phase shifting range of 0~600° was obtained and a quasi-linear 360° phase shift has been achieved at a microwave frequency of 40GHz with RF power variation lower than 2dB. A phase shift of 390° has also been demonstrated with only 1dB RF power variation using a DMRR with lower Q-factor. For variable resonance-offset operation, a continuous phase shift of 360° (270°) with only 1dB (0dB) RF power variation has also been demonstrated. Compared with the single-MRR device, the phase shifter based on a DMRR offers larger phase shifting range and more controllable RF power variation. These two advantages make the proposed device potentially useful in practical and versatile microwave applications.

Acknowledgment

This work was supported by the Danish Strategic Research Council and the EU FP7 via the projects NANO·COM and GOSPEL, respectively.

#122999 - $15.00 USD Received 25 Jan 2010; revised 26 Feb 2010; accepted 3 Mar 2010; published 11 Mar 2010